J|A|C|S
ARTICLES
Published on Web 03/30/2004

Unusual Electronic and Bonding Properties of the Zintl Phase Ca_5Ge_3 and Related Compounds. A Theoretical Analysis[1]

Anja-Verena Mudring and John D. Corbett*

Contribution from the Ames Laboratory and Department of Chemistry, Iowa State University, Ames, Iowa 50011

Received April 9, 2003; E-mail: jdc@ameslab.gov

Abstract: Theoretical reasons for metallic behavior among diverse Zintl phases have generally not been pursued at an advanced level. Here, the electronic structure of Ca_5Ge_3 (Cr_5B_3 type), which can be formulated $(Ca^{+2})_5(Ge_2^{-6})Ge^{-4}$ in oxidation states, has been explored comparatively by means of semiempirical and first-principles density functional methods. The FP-APW calculations show that alkaline-earth-metal and germanium orbitals, particularly the d orbitals on the cations and the p-π* orbitals of the halogen-like dimeric Ge_2^{-6}, mix considerably to form a conduction band. This covalency perfectly explains the unusual metallic properties of the nominally electron-precise Zintl phase Ca_5Ge_3 and its numerous relatives. Similar calculational results are obtained for Sr_5Ge_3, Ba_5Ge_3, and Ca_5Sn_3. Cation d orbitals appear to be a common theme among Zintl phases that are also metallic.

1. Introduction

Alkali as well as alkaline-earth and other dipositive metals react with many post-transition elements to form a plethora of stoichiometric/daltonide valence compounds with highly diverse structural chemistries. Historically, the Zintl border that lies between groups 13 and 14 supposedly divides the post-transition elements capable of forming Zintl compounds (to the right) from those that form truly intermetallic phases, often with substantial phase widths.[2] In general, the main structural features of these so-called Zintl phases[3] can be understood by assuming that the more electropositive components, hence the alkali, alkaline-earth, etc., metals, transfer their valence electrons to the post-transition elements which then achieve closed-shell anion states, either as isolated entities or in polyatomic arrangements. Some of the latter turn out to be isosteric with following elements and to likewise follow the octet rule, which in this special case is also referred to as the Zintl−Klemm−Busmann rule.[4]

Rationalization of the chemical bonding in other phases discovered subsequently has required that the Zintl bonding concepts be extended, for example, to include delocalized bonding in clusters analogous to that in the boranes.[5,6] Yet still, simple valence rules, building on those established by Grimm and Sommerfeld, Zintl, Klemm and Busmann, Mooser and Pearson,[7] Wade,[5] and so forth, were for many years sufficient to describe the relationship between structure and electron count perfectly.[8] All of them stress the exceptional stability of closed-shell structural units.

Generally speaking, the bonding situation in these phases is characterized by covalent interactions in the anionic (post-transition element) part of the structures, whereas ionic bonding governs the cation−anion interactions. In a traditional understanding, this behavior should lead to semiconducting or insulating properties for Zintl phases. Unfortunately, investigations of physical properties of purported Zintl phases have lagged well behind synthesis and structural studies, and only in relatively recent years has it become known that quite a number of these compounds, in disagreement with our expectations, exhibit metallic behavior. Yet as Harald Schäfer already stated: "the compounds are not able to defend themselves against our descriptions."[9] These contradictions have been exacerbated as the compounds studied approached or passed over the Zintl boundary (between groups 13 and 14) from right to left, whereupon these property criteria and, evidently, closed-shell structural descriptions began to fail frequently.[10,11] To understand the properties of these and similar Zintl versus metal-like salts, it is important to gain more in-depth knowledge about the electronic structures of these materials to learn where and why our simple views of bonding fail. Extended Hückel studies usually applied here have not been sufficient to understand many of these problems, and more thorough theoretical investigations of the electronic structures of these compounds are clearly needed.

Here, we report the first comparative theoretical study of a typical problem phase, in this case Ca_5Ge_3, using several

(1) This research was supported in part by the Office of the Basic Energy Sciences, Materials Sciences Division, U.S. Department of Energy (DOE). The Ames Laboratory is operated for DOE by Iowa State University under Contract No. W-7405-Eng-82.
(2) Zintl, E. *Angew. Chem.* **1939**, *52*, 1.
(3) Laves, F. *Naturwissenschaften* **1941**, *29*, 244.
(4) Klemm, W.; Busmann, E. Z. *Anorg. Allg. Chem.* **1963**, *319*, 297. Schäfer, H.; Eisenmann, B.; Müller, W. *Angew. Chem.* **1973**, *85*, 742.
(5) Wade, K. *Adv. Inorg. Chem. Radiochem.* **1976**, *18*, 1.
(6) Corbett, J. D. *Inorg. Chem.* **1968**, *7*, 198.
(7) Mooser, E.; Pearson, W. B. *Acta Crystallogr.* **1959**, *12*, 1015. Pearson, W. B. *Acta Crystallogr.* **1964**, *17*, 1.
(8) Kauzlarich, S. M., Ed. *Chemistry, Structure and Bonding of Zintl Phases and Ions*; VCH: New York, 1996.
(9) Schäfer, H., discussion remark, Münster, Germany, 1962; quoted in von Schnering, H.-G. *Angew. Chem.* **1981**, *93*, 44.
(10) Corbett, J. D. In *Chemistry, Structure and Bonding of Zintl Phases and Ions*; Kauzlarich, S. M., Ed.; VCH: New York, 1996; Chapter 3.
(11) Corbett, J. D. *Angew. Chem., Int. Ed.* **2000**, *39*, 670.

different approaches to gain insight as to what may give rise to metallic properties of this and related Zintl phases. Other results at this level are in process.[12−14] For a localized examination of the anionic part of the structure, we use the extended Hückel method as well as ab initio RHF calculations. To examine the properties of the extended structure and the overall electronic properties, we have carried out DFT calculations based on a full potential linear APW method as well as by the LMTO-ASA approach. An abstract for a poster describing some of this work has appeared.[15]

2. A Family of Problem Compounds

A particularly disquieting group of supposed Zintl compounds is those of a binary A_5B_3 type formed between many of the alkaline-earth-metals Ca−Ba (Ae) plus the divalent analogues Sm, Eu and the tetrels (Tt) Si, Ge, and some Sn.[16] All occur in a Cr_5B_3-type structure (below) in which one-half of the triel anions are presented as dimers, the rest as isolated and presumably closed-shell anions, $(Ae^{+2})_5(Tt_2)^{-6}Tt^{-4}$, etc., with the signs emphasizing oxidation states, not charges. Thus, these are structurally Zintl phases according to the apparent charge balance,[17] but all examples of such A_5B_3 compounds that have been examined appear to be metallic. In particular, Ca_5Ge_3 has a resistivity $\rho_{290} \simeq 170\ \mu\Omega$ cm, with a temperature coefficient of 0.32(4)% K^{-1} appropriate for a poor metal, and it as well as Sr_5Ge_3 and Sr_5Sn_3 are Pauli-paramagnetic, a characteristic of conduction electrons (or holes).[18]

3. Computational Details

To get a first, rough picture of the local bonding in the anionic structure part (Ge_2^{-6}) of Ca_5Ge_3, the extended Hückel method was used (CAESAR[20] and HyperChem[21]). Its results were compared with restricted Hartree−Fock calculations obtained from the program GAMESS.[22] Three-dimensional band structure calculations were also carried out with several programs to compare the results from semi-empirical extended-Hückel band calculations (often used for the interpretation of bonding in Zintl phases[8]) with far more precise first-principle DFT methods. The structural data employed were as reported.[16]

CAESAR. The program package CAESAR makes use of the tight-binding extended-Hückel method.[23] The Hückel parameters employed for calculations on Ca_5Ge_3 are given in the Supporting Information.

The Stuttgart LMTO Program.[24] This program follows the tight-binding linear-muffin-tin orbital (LMTO) method in the local density (LDA) and atomic sphere (ASA) approximations.[25] Interstitial spheres are introduced in the last to achieve space filling. The ASA radii as well as the positions and radii of additional empty spheres are calculated automatically. Reciprocal space integrations are carried out using the tetrahedron method.[26] The basis set of short-ranged, atom-centered TB-LMTOs contains 4s, 4p, 3d wave functions for Ca and 4s, 4p, and 4d for Ge atoms. The Ca 4p and Ge 4d orbitals are treated with the downfolding technique.[27,28] The crystal orbital Hamiltonian population (COHP) method is used for bond analysis.[29] COHP gives the energy contributions of all electronic states for selected bonds by partitioning the band structure energy, hence, the sum of energies of the Kohn−Sham orbitals, in terms of the respective orbital pair contributions. Note that the values are negative for bonding and positive for antibonding interactions, a reversal of signs used in crystal orbital overlap population (COOP[30]) diagrams in the semiempirical Hückel treatments. This difference emerges from the fact that the DOS gets multiplied by the overlap population to obtain the COOP, whereas the corresponding element of the Hamiltonian is used to weight the DOS in the case of COHP.

WIEN2k. The WIEN2k[31] code has implemented the full-potential linearized augmented plane wave method (FP-APW) with local orbitals (lo).[32] For treatment of the electron correlation within the generalized gradient approximation, the electron exchange-correlation potential is used with the parametrization by Perdew et al.[33] We have treated Ca 1s/2s/2p and Ge 1s/2s/3s/3p as core states; a value of 2.0 Å was chosen as the muffin-tin (MT) radii for both elements. For valence states, relativistic effects are included through a scalar relativistic treatment,[34] and core states are treated fully relativistic.[35] To illustrate the particular orbital character of bands, the fatband representation is used in which bands are drawn with a thickness representative of the contribution of the corresponding orbitals.

In all cases, the Fermi energy is chosen as the internal reference. The structural and orbital parameters employed for Ca_5Ge_3 are given in the Supporting Information.

4. Results and Discussion

Typical Zintl phases are characterized by low energy electronic states centered on the anionic structure portion that are completely occupied by electrons. States contributed by cations are in general of higher energy and thus empty and usually ignored. Typically, this electronic configuration gives rise to a band gap, and some Zintl phases examined are indeed semiconductors.[8] Yet other Zintl phases exhibit metallic properties although they apparently follow the Zintl−Klemm−Busmann guidelines or later rules for electron counts in "electron-deficient" polyhedra.[10] One of these examples is Ca_5Ge_3.

The well-known (hydrogen-free) Zintl phase Ca_5Ge_3[16] crystallizes with the Cr_5B_3 structure type, Figure 1, which can be viewed as a 1:1 intergrowth of two types of structural elements along the crystallographic c axis. That at about $z = 0$, $^1/_2$ is

(12) Li, B.; Mudring, A.-V.; Corbett, J. D. *Inorg. Chem.* **2003**, *42*, 6940.
(13) Guloy, A. M.; Mudring, A.-V.; Corbett, J. D. *Inorg. Chem.* **2003**, *42*, 6673.
(14) Mudring, A.-V.; Corbett, J. D., unpublished research.
(15) Mudring, A.-V.; Corbett, J. D. *Z. Anorg. Allg. Chem.* **2002**, *628*, 2226.
(16) Leon-Escamilla, E. A.; Corbett, J. D. *J. Solid State Chem.* **2001**, *159*, 149.
(17) The foregoing group and all of the other Sn, Pb analogues also exist as isotypic (stuffed) ternary hydrides Ae_5Tt_3H, which implies more problems with the simple picture because the supposed closed-shell anions have evidently been oxidized by hydrogen.[18] The structure parameter shifts on oxidation of Ca_5Ge_3 to Ca_5Ge_3H are distinctive and evidently affected an earlier structural study.[19]
(18) Leon-Escamilla, E. A.; Corbett, J. D. *Inorg. Chem.* **2001**, *40*, 1226.
(19) Eisenmann, B.; Schäfer, H. *Z. Naturforsch.* **1974**, *29B*, 460.
(20) Ren, J.; Liang. W.; Whangbo, M.-H. CAESAR; PrimeColor Software, Inc.: Raleigh, NC, 1998.
(21) HyperChem Professional Release 7; Hypercube, Inc.: Gainesville, FL, 2001.
(22) Gordon, M. GAMESS; Iowa State University.
(23) Whangbo, M. H.; Hoffmann, R.; Woodward, R. B. *Proc. R. Soc. London* **1979**, *A366*, 23. Hoffmann, R. *J. Chem. Phys.* **1963**, *39*, 1397.
(24) Tank, R. W.; Jepsen, O.; Burckhardt. A.; Andersen, O. K. *TB-LMTO-ASA Program*, Vers. 4.7; Max-Planck-Institut für Festkörperforschung: Stuttgart, Germany, 1998.
(25) Skriver, H. L. *The LMTO Method*; Springer-Verlag: Berlin, Germany, 1984. Jepsen, O.; Sob, M.; Andersen, O. K. *Linearized Band-Structure Methods in Electronic Band-Structure and its Applications*; Springer Lecture Note; Springer-Verlag: Berlin, Germany, 1987. Andersen, O. K.; Jepsen, O. *Phys. Rev. Lett.* **1984**, *53*, 2571.
(26) Andersen, O. K.; Jespen, O. *Solid State Commun.* **1971**, *9*, 1763. Blöchl, P.; Jepsen, O.; Andersen, O. K. *Phys. Rev. B* **1994**, *34*, 16223.
(27) Lambrecht, W. R. L.; Andersen, O. K. *Phys. Rev. B* **1986**, *B34*, 2439.
(28) Jepsen, O.; Andersen, O. K. *Z. Phys. B* **1995**, *B97*, 35. Krier, G.; Jepsen, O.; Andersen, O. K. Max-Planck-Institute fur Festkörperforschung, Stuttgart, Germany, unpublished.
(29) Dronskowski, R.; Blöchl, P. *J. Phys. Chem.* **1993**, *97*, 8617.
(30) Hughbanks, T.; Hoffmann, R. *J. Am. Chem. Soc.* **1983**, *105*, 3528.
(31) Blaha, P.; Schwarz, K.; Madsen, G. K. H.; Kvasnicka, D.; Luitz, U. *WIEN2k*, An Augmented Plane Wave + Local Orbitals Program for Calculating Crystal Properties (Karlheinz Schwarz, Technical Universität Wien, Austria), 2001. ISBN 3-9501031-1-2.
(32) Singh, D. J. *Planewaves, Pseudopotentials, and the APW Method*; Kluwer Academic Press: Boston, MA, 1994; Blaha, P.; Schwarz, K.; Soratin, P.; Trickey, S. B. *Comput. Phys. Commun.* **1990**, *59*, 399.
(33) Perdew, J. P.; Burke, S.; Ernzerhof, M. *Phys. Rev. Lett.* **1996**, *82*, 3865.
(34) MacDonald, A. H.; Pickett, W. E.; Koelling, D. D. *J. Phys. Chem.* **1980**, *C13*, 2675.
(35) Desclaux, J. P. *Comput. Phys. Commun.* **1969**, *1*, 216.

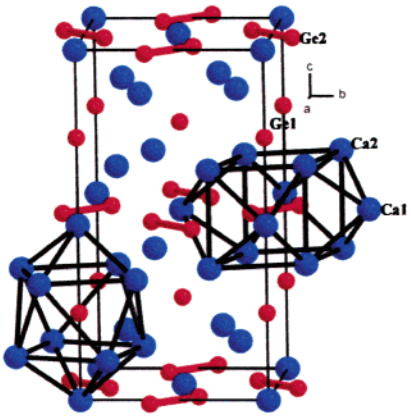

Figure 1. Structure of Cr_5B_3 with atom identities; Ca in blue, Ge in red. Cationic coordination polyhedra around the anionic dimer and monomer units are highlighted.

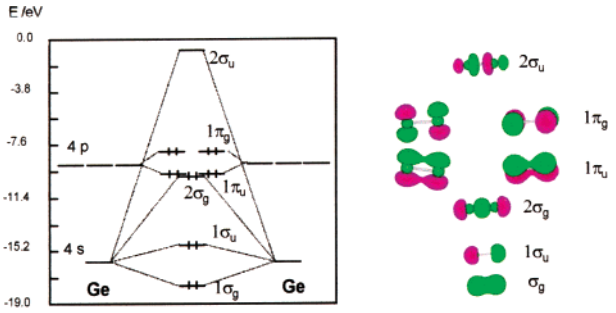

Figure 2. Molecular orbital diagram for Ge_2^{-6} obtained from extended Hückel calculations: energy niveaus (left) and corresponding molecular orbitals (right).

characterized by anionic Ge2 dimers (red) surrounded by rhomboidal prisms of Ca2 that are capped on all rectangular faces by Ca1, as is outlined in blue. In the other part around $z = {}^1/_4, {}^3/_4$, there are Ge1 monoanion-centered square antiprisms of Ca2 that are in turn capped by Ca1 on two faces along $\vec{c}$, as is also highlighted. (Note that there is a 2:1 proportion of Ca2:Ca1 in the whole structure.) These atom identities will aid later understanding. As a salt, the very similar heteroatomic distances in the compound are about as expected for interionic contacts: Ca2−Ge1, 2.28 Å (×8), and Ca−Ge2 (dimer), 3.06−3.13 Å (×8), the longer being about the waist to Ca1. The Ge2−Ge2 dimer separation in this environment is 2.575 Å, typical relative to analogous phases containing Si or Sn.

The structure of Ca_5Ge_3 can be seemingly understood on the basis of the classical Zintl concept by applying the $(8 - N)$ rule for electron count: $(Ca^{+2})_5(Ge_2^{-6})(Ge^{-4})$. Hückel calculations confirm the dimeric (Ge_2^{-6}) unit to be isosteric with Br_2 (Figure 2), and RHF calculations give comparable results. Because closed-shell configurations appear to be achieved for all ions, Ca_5Ge_3 as a valence compound is expected to be a diamagnetic semiconductor, but property measurements show the compound to be metallic and Pauli-paramagnetic.[16]

The question comes up as to what gives rise to the metallic properties of Ca_5Ge_3. Perhaps Ge^{-4} is not able to stabilize four negative charges, or the higher lying and nominally occupied π^* orbitals on the (Ge_2^{-6}) dimers instead form a conduction band that extends over the whole crystal. (Intuitive concern about the status of these states has been expressed before.[16]) Also, the assumption of complete electron transfer from the cations onto germanium may be an exaggeration; rather, some

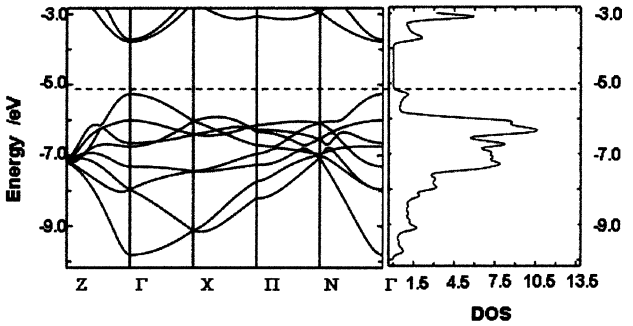

Figure 3. Band structure (left) and density of states (right) for Ca_5Ge_3 obtained from Hückel calculations. Dotted line signifies the Fermi energy.

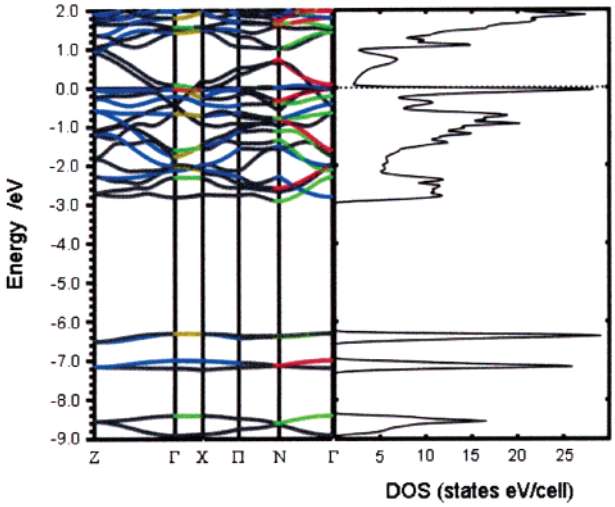

Figure 4. Band structure (left) and density of states (right) for Ca_5Ge_3 obtained from FP-APW calculations. Dotted line signifies the Fermi energy.

electron density may remain on calcium or get delocalized into some sort of a conduction band, or the calcium cations may polarize the soft, highly charged germanium anions and give rise to substantial nonionic interactions and the formation of mixed bands.

In the case of Ca_5Ge_3, standard extended Hückel calculations of the sort that commonly afford simple and useful understanding of bonding in comparable compounds[8] back our simple view of the Zintl character as they show the Fermi energy of Ge_2^{-6} to be located within an energy gap of −1.3 eV (Figure 3), but they fail to explain the true properties of Ca_5Ge_3. However, semiempirical methods such as extended Hückel can easily fail because of several reasons: strong Coulomb interactions and uncertainties in the relative values of the parameters for the alkali or nonalkali elements as well as for the post-transition elements may seriously influence the degree of orbital mixing and interaction. This holds true even after iterating the atom parameters to charge consistency in intermetallic phases. As a consequence, further efforts have been undertaken to understand the origin of metallic conduction in Ca_5Ge_3 with the aid of the more elaborate theoretical approaches via TB-LMTO-ASA and APW-GGA-DFT calculations.

DFT band structure calculation results in Figure 4 for Ca_5Ge_3 from the WIEN2k program clearly show, in contrast to simple extended-Hückel calculations, that the Fermi energy falls in a region with a substantial density of states (DOS), and, correspondingly, several bands cross the Fermi level. Significant

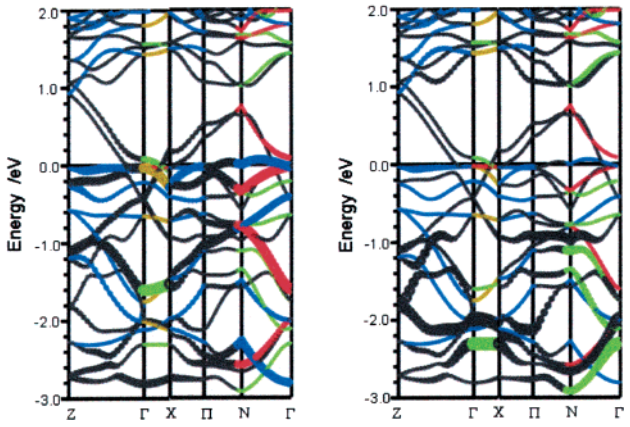

Figure 5. Band structure for Ca_5Ge_3 over the valence band region, as obtained from FP-APW calculations with fatband representations for Ge2 p_x (left) and Ge2 p_y (right).

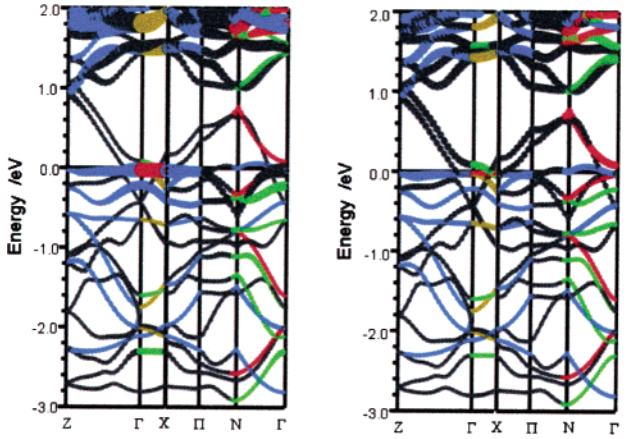

Figure 6. Band structure for Ca_5Ge_3 over the valence band region, as obtained from FP-APW calculations; fatband representations for Ca1 d (left) and Ca2 d (right).

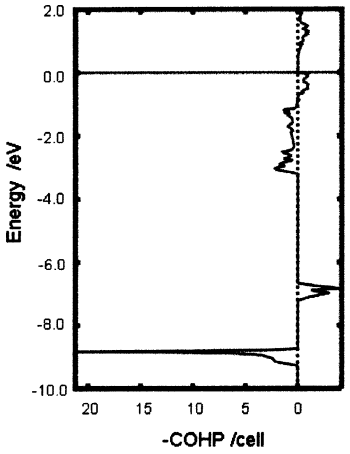

Figure 7. COHP analysis for the Ge2−Ge2 interaction in Ge_2^{-6} over the entire energy window, as obtained from LMTO-ASA calculations. Plotted is the negative COHP per/cell; thus bonding interactions are indicated by positive numbers.

cation mixing into germanium states (covalency) is evident. The WIEN2k code seems to allow a far more accurate interpretation of the (relative) energies, whereas the Stuttgart LMTO-ASA program yields a smaller density of states at the Fermi level (see Supporting Information) because of its inherent approximations, presumably in the potential and in the atomic spheres assigned in a highly directional bonding situation. In fact, the augmented plane wave method of the former has proven to be one of the most accurate methods for the computation of the electronic structure of solids within density functional theory.[31] Therefore, the results of the LMTO-ASA calculations have been utilized only for the interpretation of bonding through COHP analyses as the WIEN2k code does not support such an analysis. All other interpretations, that is, fatband analyses, are based on the results of the WIEN2k calculations.

The band structure and DOS for Ca_5Ge_3 show two distinctively different regions. A lower region with localized states originates predominantly from germanium s states, and an upper region with highly dispersed bands around the Fermi level originates mainly with Ge p states, whereas cation levels just above E_F are largely Ca 3d. The latter two sets of orbitals are responsible for the metallic character of Ca_5Ge_3. Detailed analyses reveal the orbital contributions of different atoms to these bands and states, and these will be illustrated by some fatband representations of the band structure.

Analyses of these for the Ge_2^{-6} dimer in Figure 5 indicate substantial contributions at the Fermi level from p_x and p_y orbitals on Ge2 which in the localized picture of a Ge_2^{-6} anion correspond to the π^* orbitals (Figure 2). (To comply with the local point group symmetry, a coordinate system is chosen with p_x parallel to the crystallographic *c*). The p_z orbitals that form a σ bond along the Ge−Ge bonding axis are of lower energy and thus make no contributions here. Analogous analysis of the band structure for the Ge^{-4} monomer also shows substantial contributions at the Fermi level from p orbitals, but these are less pronounced than those in the dimer (see Supporting Information, Figure S2).

The fatbands for the d orbitals on the two Ca atom types make it obvious that the more numerous Ca2 are contributing more states at the Fermi level, Figure 6, in part because these atoms are 8 of the 10 or 12 close neighbors about each of the anions. To check the interaction between Ca2 and the Ge anions, crystal overlap Hamiltonian population analyses (COHP) were also carried out. Those within Ge2 (dimer) are in agreement with the localized view of a Ge_2^{-6} unit, Figure 7, in which σ, σ^*, σ, π, and π^* orbitals or states are filled, whereas σ^* and most d orbitals lie above the Fermi level. Yet COHP analyses of the Ca−Ge interactions show significant bonding around the Fermi level for the Ge1 monomer as well as for the Ge2 dimer. Otherwise, it is not possible to distinguish which particular d orbitals on the cations are more important as these are quite diffuse. The germanium monomer possesses, in general, low-lying filled states as expected for an isolated Ge^{-4}, but bands with significant p_x and p_y contributions from Ge1 cross the Fermi level very steeply too (Supporting Information). The *p* states arising from the dimer are located around the Fermi level, and the bands exhibit only a slight dispersion. In a more localized view, they can be regarded as the π orbitals of $[Ge-Ge]^{-6}$ formed by the p_x and p_y orbitals. On the other hand, Ca d orbitals mix appreciably with the germanium states. Empty Ca d states fall in the region of the Fermi level, and Ca2 states overlap especially well with anion states, Figure 8 (note the scale change). They not only show a high contribution to the bands but are also highly dispersed. Thus, it is the cations that are mainly responsible for mixing with and dispersion of anion p states above the anion-only Fermi level, leading to the loss of a band gap and the metallic behavior of Ca_5Ge_3.

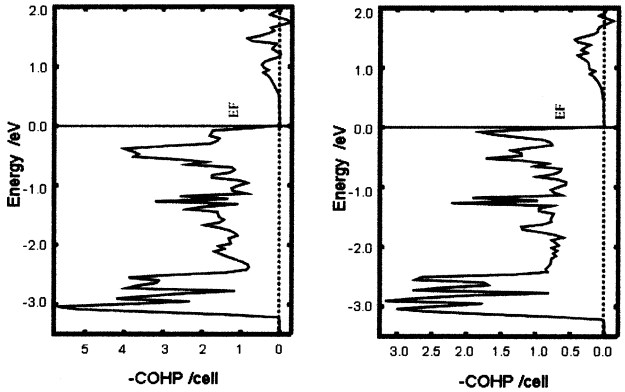

Figure 8. COHP analysis for the Ca1−Ge2 (left) and Ca2−Ge2 (right) interactions over the valence band region for Ca_5Ge_3 obtained from LMTO-ASA calculations.

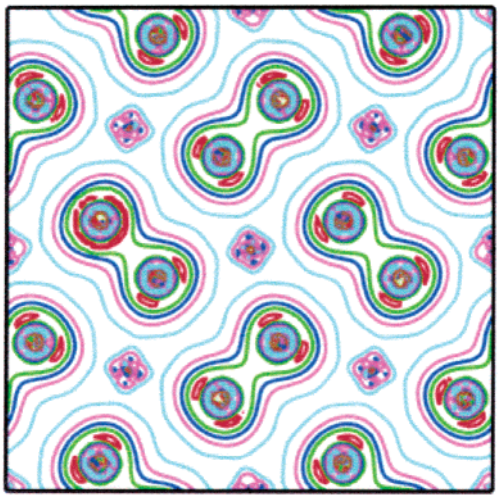

Figure 9. Electron density plot about Ca1 and Ge_2^{-6} in the (002) plane.

Overlap of empty Ca states with Ge p states for orbitals on the dimer also leads to a depopulation of its antibonding π^* orbital. Therefore, the Ge−Ge bond has more of a partial double bond character. Electron density plots show a substantial electron density between the Ge2 atoms and slight mutual distortions of electron density toward the other neighboring ions, Figure 9. The Ge monomer exhibits a nearly spherical electron density. It is noteworthy that the cation−anion mixing in thse structure types increases on replacement of Ca by Sr and then by Ba. The cation d levels come down in energy in the same order, whereas the polarizing power of the cation decreases. The same general picture also applies to Ca_5Sn_3 according to equivalent calculations. Also, in all cases, the oxidation of stable Ae_5Tt_3 phases to Ae_5Tt_3Z, Z = H, F, is observed to shorten the Tt2−Tt2 bond[16] as some antibonding states near E_F in the former are emptied.

Our parallel studies of bonding in other Zintl-like compounds and the questions raised by their metal-like characteristics show that appreciable d-orbital mixing of alkaline-earth or rare-earth metal cations with anion states is a common and frequent message. Thus, an absence of closed Pb^{-4} bands gives stability and metallicity to a series of Ca_5Pb_3Z (stuffed Mn_5Si_3) phases in which Z is a 3d metal, and likewise for Li_2MgPb and inverse perovskitic Ca_3PbO (but not for Ca_3PbH_2, for reasons of symmetry).[14] These events do not occur for tin as far as is known; there are no equivalent Ca_5Sn_3 (Mn_5Si_3 type) phases, for example. The existence of stoichiometric but e-deficient Ae_4Bi_3 phases for Ae = Sr, Ba (but not for Sb) also result from strong mixing of Ae d orbitals with Bi p orbitals to give an open band. These d-orbital effects are often not adequately described by extended Hückel methods, and the same is true of the anion states in the nominal Zintl compounds A_3Pn, A = K, Rb, Cs, Pn = Sb, Bi.[14] However, similar but sometimes more extreme effects of cation d states on and covalency with Sr, Ba (Ae), and, especially, La are evident even at the extended Hückel level for the metallic, cation-poorer Ae_3Tt_5 (Tt = Sn, Pb) and La_3In_5 cluster phases.[36]

The d-mixing is not sufficient to produce a universal metallic behavior; rather, such effects naturally also depend on the structures and on the polarizability of and valence energies for the polyatomic anion pardners. Thus, Ca_2Ge and Ca_2Pb (inverse $PbCl_2$ type) are semiconductors according to ab initio theory,[37] whereas the metallicity of CaGe[38] is not surprising considering its CrB-type structure. The foregoing $\pi-\pi^*$ effects for all Cr_5B_3-type examples are expected to be general, and the binaries that have been measured (Ca−Ge, Sr−Ge, Sr−Sn) are all metallic. Yet a tetrel π system with calcium is not sufficient: $Ca_{31}Sn_{20}$, which contains formal Sn^{-4}, Sn_2^{-6}, and linear Sn_5^{-12} (singly bonded) units, is diamagnetic and therefore probably a semiconductor.[39]

To summarize, modified Zintl−Klemm−Busmann concepts are able to describe the more general features of the anionic structure parts as well as the number and character of valence orbitals in these compounds, comparable to the well-known isolobal concept in organic chemistry, but the assumed electron transfer is often far overestimated and mixing is ignored. Here, interactions between the anionic and the cationic parts of the structure also play an important role. In the end, these interactions determine decisively the properties of Ca_5Ge_3, making it metallic. Similar perturbations presumably affect most and probably all other binary A_5Tt_3 compounds that have this structure. Also, the existence of many examples of corresponding A_5Tt_3Z phases with Z = H or F that are also metallic[16,18] is no longer anomalous.

Acknowledgment. A.-V.M. thanks the A. v. Humboldt Foundation, Bonn, Germany, for a Feodor Lynen Fellowship.

Supporting Information Available: Hückel and crystallographic parameters for Ca_5Ge_3, plots of the LMTO-ASA results for Ca_5Ge_3, a fatband representation for p orbitals on Ge^{-4}, and the corresponding projected DOS result (Wien2k) (PDF). This material is available free of charge via the Internet at http://pubs.acs.org.

JA030216B

(36) Klem, M. T.; Vaughey, J. T.; Harp, J. G.; Corbett, J. D. *Inorg. Chem.* **2001**, *40*, 7020.
(37) Migas, D. B.; Miglio, L.; Shaposhnikov, V. L.; Borisenko, V. E. *Phys. Rev. B* **2003**, *67*, 205203.
(38) Evers, J.; Weiss, A. *Solid State Commun.* **1975**, *17*, 41.
(39) Ganguli, A. K.; Guloy, A. M.; Leon-Escamilla, A. E.; Corbett, J. D. *Inorg. Chem.* **1993**, *32*, 4349.